Electronic Supplementary Material (ESI) for Soft Matter.

Supplementary Information for

Single-molecule Lamellar Hydrogels from Bolaform Microbial Glucolipids

Ghazi Ben Messaoud, Patrick Le Griel, Sylvain Prévost, Daniel Hermida-Merino, Wim Soetaert, Sophie L. K. W. Roelants, Christian V. Stevens, Niki Baccile*

Correspondence to: niki.baccile@sorbonne-universite.fr

This PDF file includes:

Figs. S1 to S6

References for SI reference citations

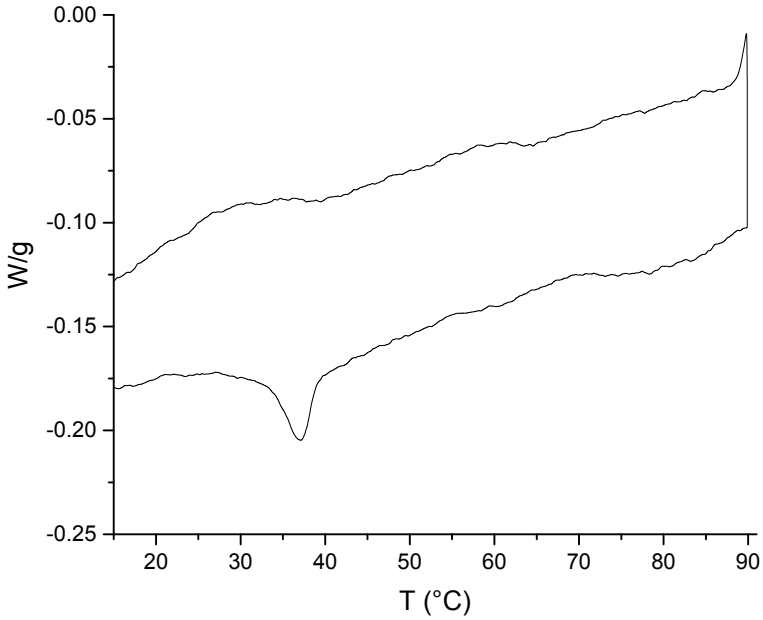

Figure S 1 – Differential Scanning Calorimetry (DSC) thermogram of the native G-C18:0 powder acquired at 1°C/min

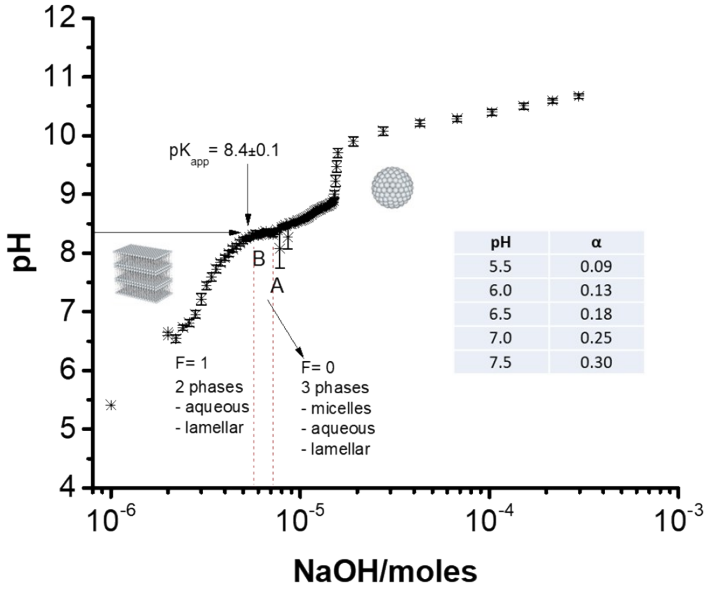

Figure S 2 – Experimental determination of the apparent pKa of glucolipid G-C18:0 by titration using NaOH in water at T= 25°C (titrated volume: 1.8 mL). The ionization degrees are estimated using the Gibb's free energy rule applied to lamellar phases composed of fatty acids[1]

Estimating the ionization degree, α, for fatty acids as a function of pH is a long-date challenge which faces the problem of liquid-solid transition and coexistence of multiple phases. The problem of calculating α is in fact the problem of estimating the pKa. For stearic acid (which composes the fatty backbone of G-C18:0), the molecular pKa measured in organic solvents is between 4.9 and 5,[2] but this value varies between 5 and 7.6 when stearic acid is contained in a micellar environment in water.[3] In this work, we use the method of Cistola et al.[1], who applied the Gibb's phase rule to the titration curve of selected fatty acids below and above the melting temperature of the aliphatic chain. The advantage of this approach is multiple: 1) it is simple; 2) it has been used on the micelle-to-lamellar phase transitions of fatty acids in water; 3) it can be applied on our own experimental data (the titration curve) on a similar system. For the detailed description of the method, one can refer to ref. [1]. In this work, the region between points A and B in Figure S 2 satisfies the condition of invariance (F= 0), where composition is fixed, while the region below B (pH= 8.3) is characterized by one degree of freedom (F= 1), where composition of the lamellar phase can vary. α is estimated between pH 5 and pH 8.3, where α= 0.5 at B.

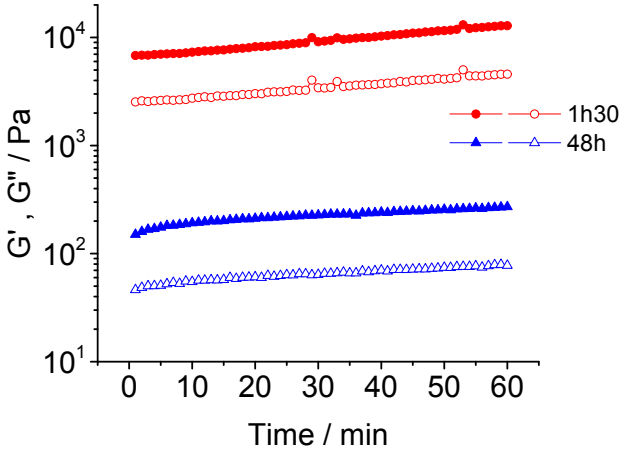

Figure S 3 – Time evolution of G' (full symbols) and G'' (open symbols) (ω= 6.28 rad.s^{-1} and γ= 0.05 %) for G-C18:0 ($C_{G\text{-}C18:0}$ = 5 wt%, pH= 6.7, [NaCl]= 167 mM) after 1h30 and 48 h from thermal annealing. Plate-plate geometry (25 mm), imposed normal force (NF = 0 N) and initial gap (0.5 mm).

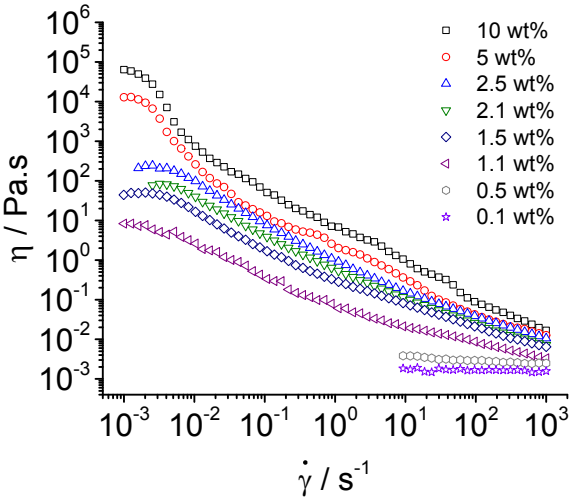

Figure S 4 – Shear thinning profiles showing the evolution of viscosity with shear rate at different G-C18:0 concentrations at pH= 6.7 ± 0.1 and [NaCl]= 163 mM. Plate-plate geometry (25 mm) and an imposed gap of 0.5 mm are used

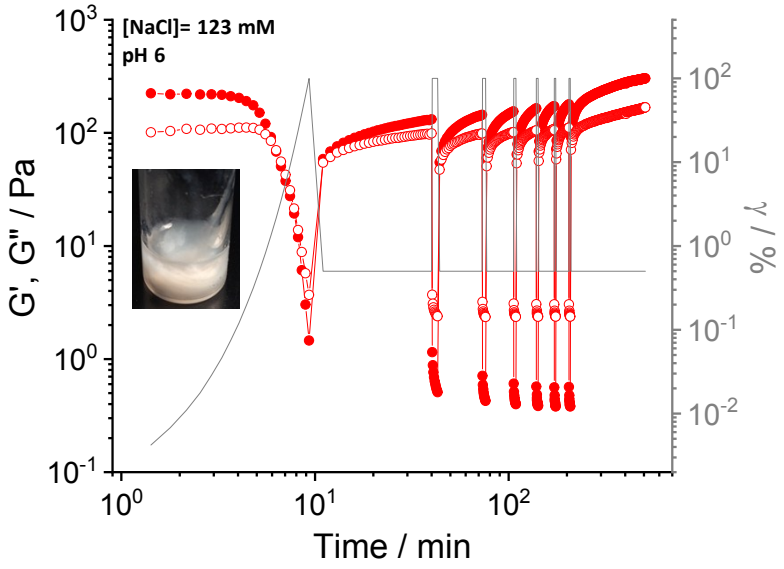

Figure S 5 – Time evolution of G' (full symbols) and G'' (empty symbols) with the imposed shear strain (γ) at angular frequency (ω= 6.28 rad·s^{-1}). Logarithmic increase of the shear strain (4·10^{-3} < γ < 100 %) during 10 min followed by a recovery at γ = 0.5 % (upper limit of the LVER) during 30 min, followed by 6 cycles of step strain experiments (γ = 100% during 2 min followed by γ = 0.5 % during 30 min (during the first 5 cycles) and 300 min in the last cycle. Plate-plate geometry (25 mm) and an imposed normal force (NF = 0 N) with an initial gap (0.5 mm) are used.

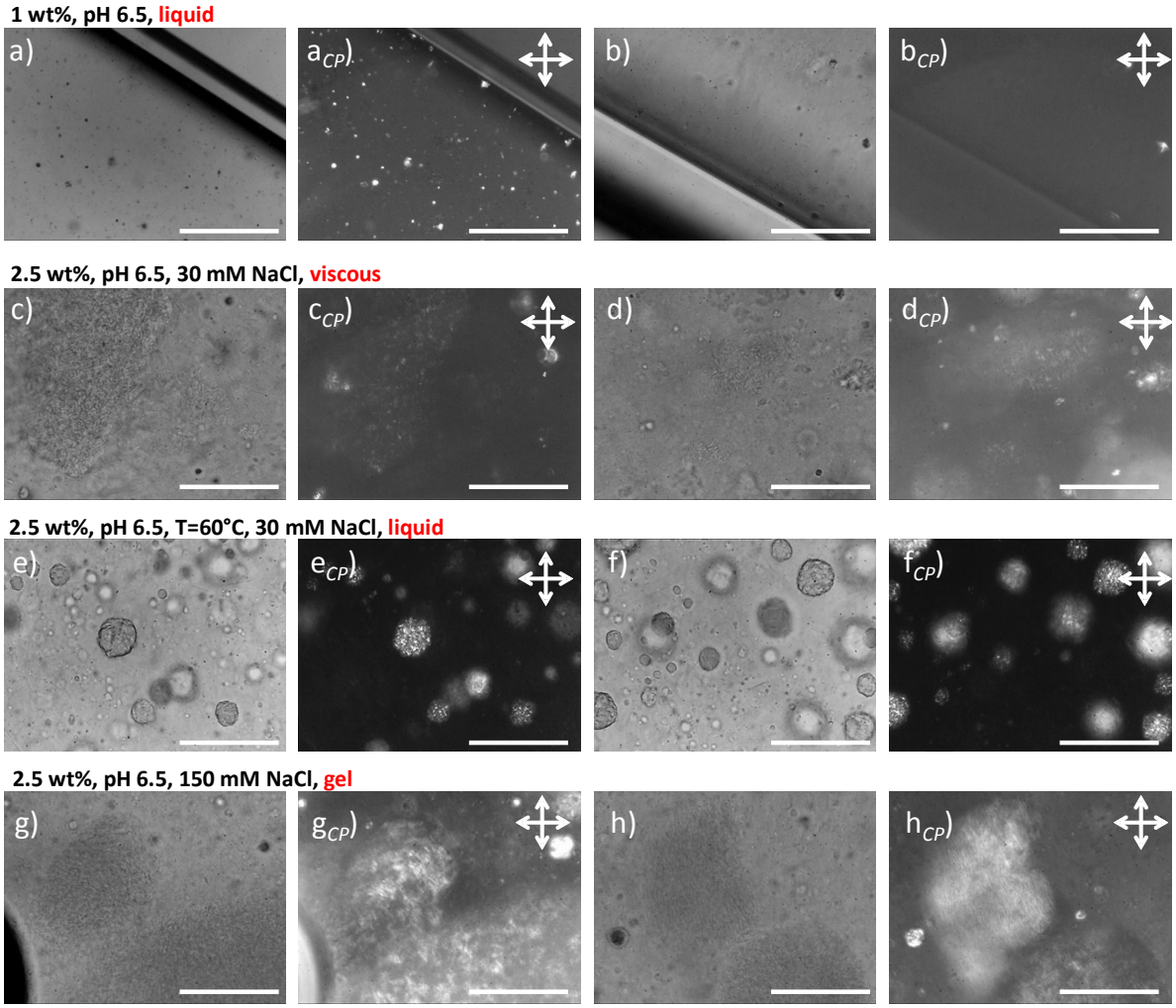

Figure S 6 – Bright Field and polarized light microscopy (*CP*: Crossed Polarizers) images of a set of G-C18:0 samples at pH 6.5 in water (scale bar: 100 µm). Samples are prepared in flame-sealed flat capillary of 200 µm thickness, as in ref. [4]. Exact conditions are given on top of each series of images. All images are recorded after 24 h from preparation. All samples are kept at room temperature ~ 23°C, except in images e)-f), in which samples are kept at T= 60°C. The physical state of the sample are explained in red for each series of images. Images in c)-d) and e)-f) refer to the same sample, although in e)-f) the sample has been placed at T= 60°C.

Considerations on the lamellar phase

Nematic phases are characterized by orientational order and loss in translational order, and the latter could be promoted by the development of defects, like screw dislocations. Dhez *et al*. have shown the effect of dislocation defects on the diffraction profile of a lamellar phase close to the lamellar-to-nematic transition in lipid-surfactant-water systems, pointing at the complexity of a straightforward attribution of SAXS profiles under these conditions.[5] SAXS is commonly employed to characterize the lamellar nature of a lipid phase, however, the diffraction peak alone in the SAXS/SANS data in the G-C18:0 hydrogels is often very broad and it may not unambiguously help to discriminate between nematic order and a defectuous lamellar phase,[5,6] especially for the viscous solutions at low ionic strength lacking of a second order peak. The $d_{(100)}$ peak is much broader (Figure 2 in the main text) than what one classically finds in lamellar phases, and it could be interpreted as a coagel-to-gel transition[7] or to a nematic phase.[6] The former case is excluded, because the characteristic fibrillar crystals are never observed and gel always forms below the lipid T_m. Concerning the presence of a nematic phase, the SAXS data of hydrogels (e.g., pH 7, [NaCl]≤ 250 mM, Figure 2d in the main text) can be fitted with a lamellar form factor, while the diffuse scattering peak below 1 nm^{-1} can be fitted with a lamellar structure factor taking into account displacement fluctuations about the ideal lattice position.[8] Analogous SAXS profiles are also reported for biomembranes.[9] Meanwhile, all cryo-TEM data in our possession show the systematic presence of flat sheets being "infinite" in the planar dimension and polarized light microscopy data never display any typical texture of nematic order but they all rather closely look like the whispy textures found in lamellar hydrogels, as commented in the main text.

References

1 D. P. Cistola, J. A. Hamilton, D. Jackson and D. M. Small, *Biochemistry*, 1988, **27**, 1881–1888.

2 J. R. White, *J. Am. Chem. Soc.*, 1950, **72**, 1859–1860.

3 M. Ptak, M. Egret-Charlier, A. Sanson and O. Bouloussa, *Biochim. Biophys. Acta - Biomembr.*, 1980, **600**, 387–397.

4 H. E. Warriner, P. Davidson, N. L. Slack, M. Schellhorn, P. Eiselt, S. H. J. Idziak, H. W. Schmidt and C. R. Safinya, *J. Chem. Phys.*, 1997, **107**, 3707–3722.

5 O. Dhez, S. Köig, D. Roux, F. Nallet and O. Diat, *Eur. Phys. J. E*, 2000, **3**, 377–388.

6 P. Davidson, C. Penisson, D. Constantin and J.-C. P. Gabriel, *Proc. Natl. Acad. Sci.*, 2018, **115**, 6662–6667.

7 E. Carretti, V. Mazzini, E. Fratini, M. Ambrosi, L. Dei, P. Baglioni and P. Lo Nostro, *Phys. Chem. Chem. Phys.*, 2016, **18**, 8865–8873.

8 F. Nallet, R. Laversanne and D. Roux, *J. Phys. II*, 1993, **3**, 487–502.

9 A. Steiner, P. Szekely, O. Szekely, T. Dvir, R. Asor, N. Yuval-Naeh, N. Keren, E. Kesselman, D. Danino, R. Resh, A. Ginsburg, V. Guralnik, E. Feldblum, C. Tamburu, M. Peres and U. Raviv, *Langmuir*, 2012, **28**, 2604–2613.